Supplement of: European runoff drought typology: historical classification and projected changes under RCP 4.5

Sadaf Nasreen[1], Oldrich Rakovec[1], Rohini Kumar[2], Ujjwal Singh[1], Petr Maca[1], Yannis Markonis[1], and Martin Hanel[1,3]

[1]Faculty of Environmental Sciences, Czech University of Life Sciences Prague, Praha-Suchdol 16500, Czech Republic
[2]UFZ-Helmholtz Centre for Environmental Research, Leipzig 04318, Germany
[3]T.G. Masaryk Water Research Institute, Podbabska 30, Praha 6, 16000, Czech Republic

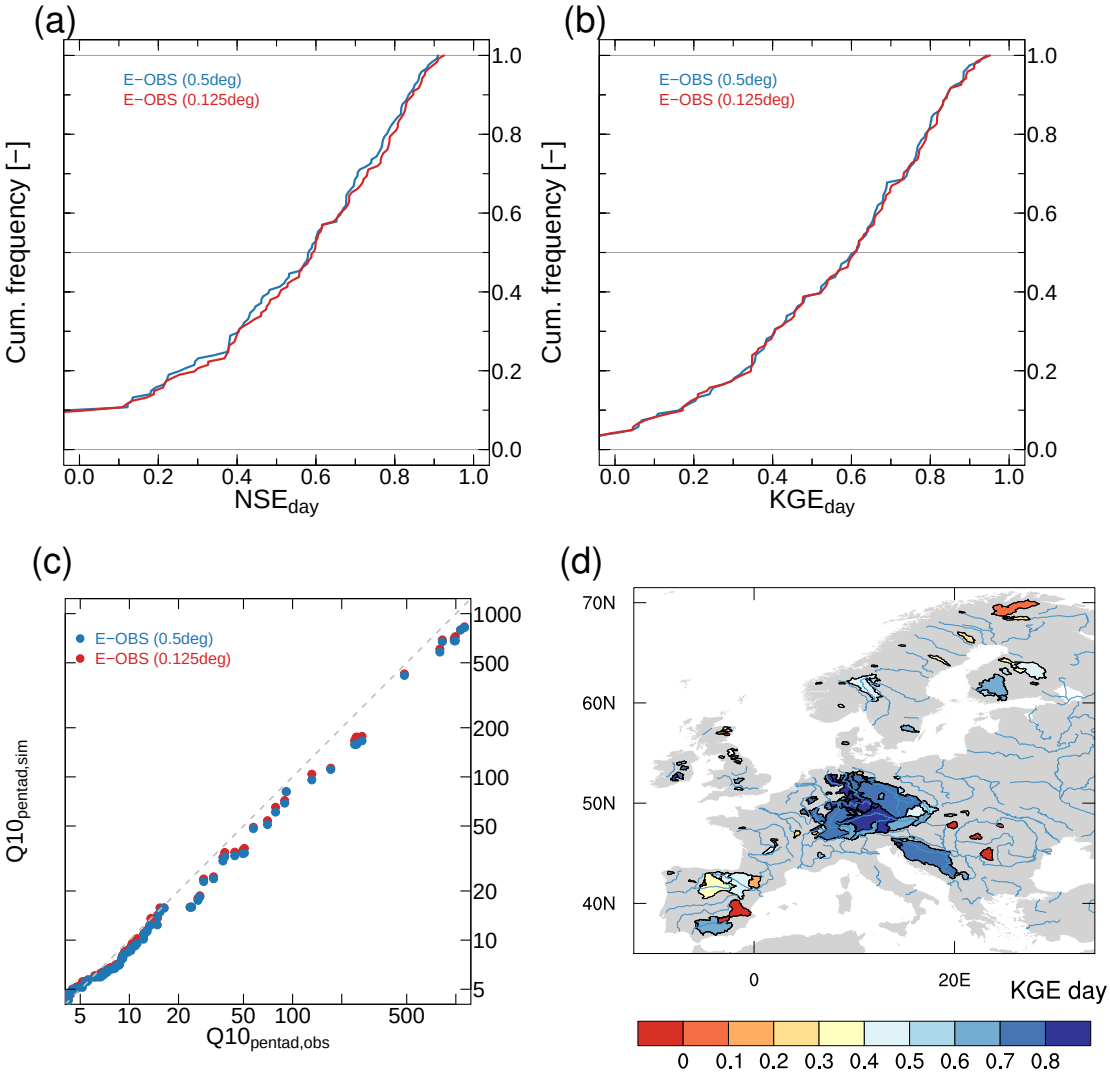

Figure S1. Evaluation of daily streamflow simulations from mHM for GRDC basins (n=123) driven by E-OBS for period 1982-2016. Panels (a) and (b) show cumulative distributions of the Nash-Sutcliffe Efficiency (NSE) and Kling–Gupta Efficiency (KGE), respectively, for two distinct hydrological spatial resolution (0.5°x0.5° and 0.125°x0.125°). Panel (c) presents the scatter plot of 10th percentile streamflow (Q10, pentad scale) between GRDC observations and mHM simulations. Panel (d) shows the spatial distribution of the 123 basins used in the model evaluation showing daily KGE.

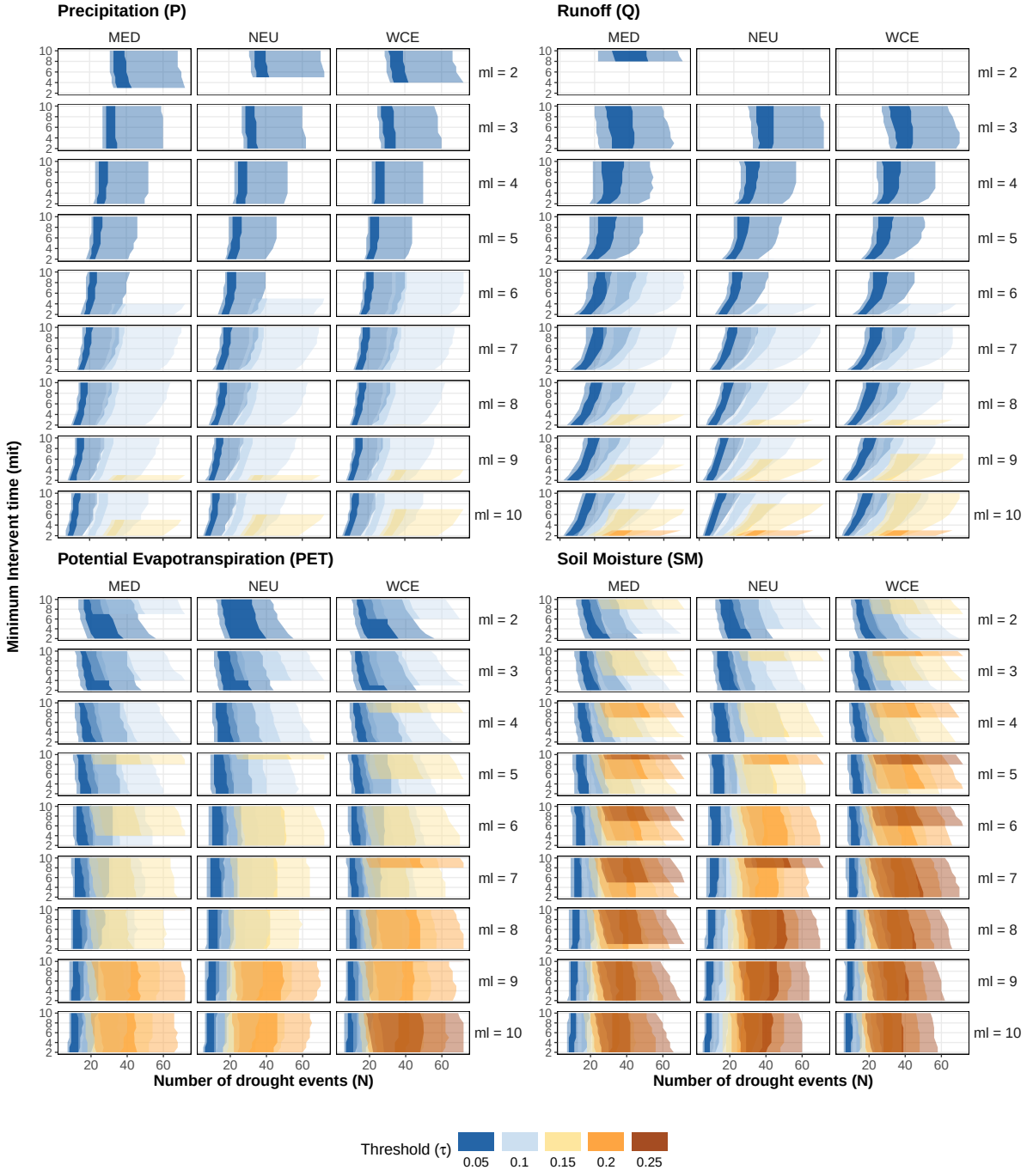

Figure S2. Number of drought events (N) across hydrological variables (P, PET, Q, SM) and IPCC regions (MED, NEU, CEU) for different severity thresholds (tau), minimum durations (ml), and minimum inter-event times (mit). Ribbons show 25th–75th percentiles (dark) and 10th–90th percentiles (light).

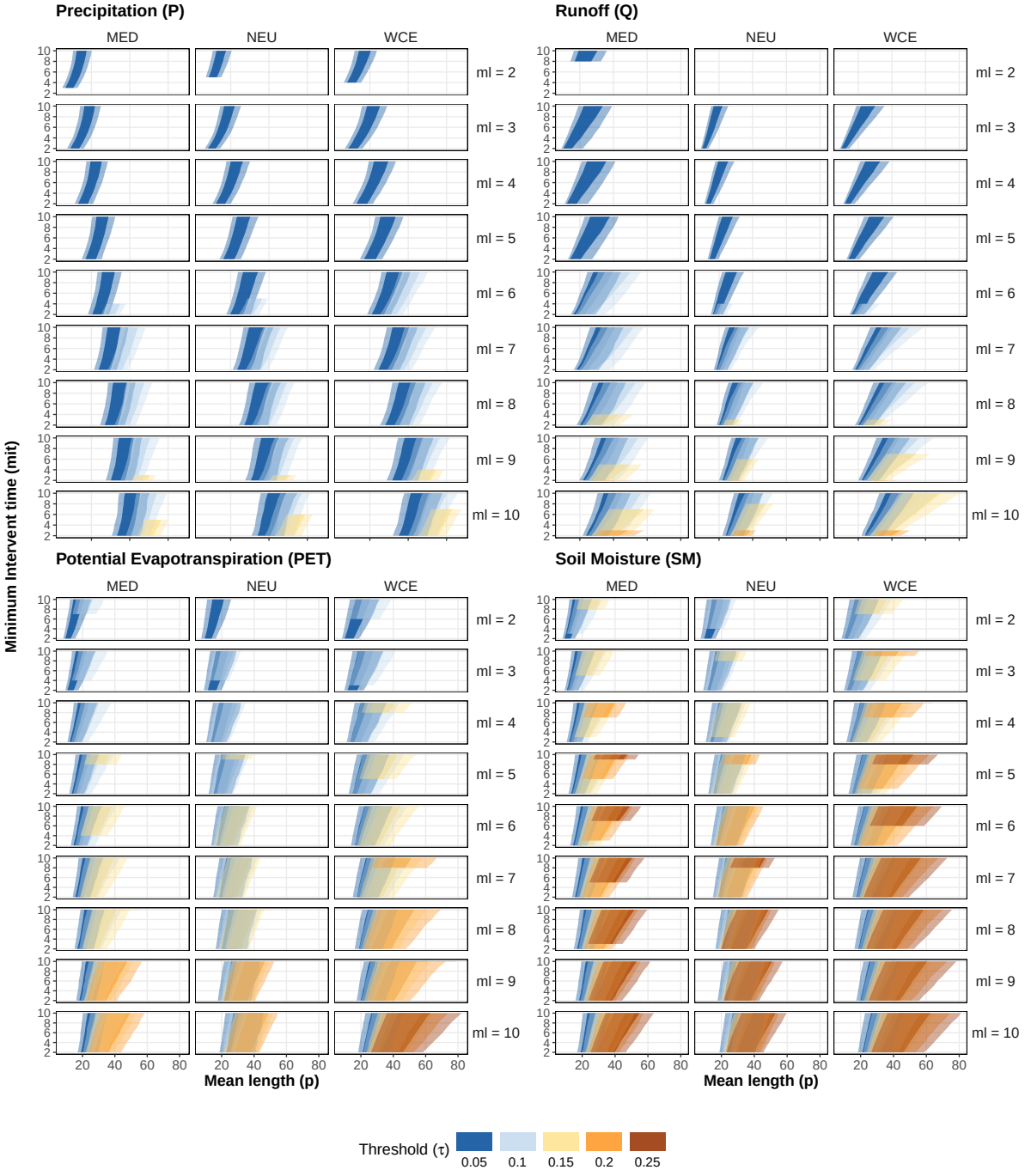

Figure S3. Mean drought duration (p) across hydrological variables (P, PET, Q, SM) and IPCC regions (MED, NEU, CEU) for different severity thresholds (tau), minimum durations (ml), and minimum inter-event times (`mit`). Ribbons show 25th–75th percentiles (dark) and 10th–90th percentiles (light).

Table S1. Comparison of average duration between GCMs (RCP4.5) and EOBS (1971–2000), categorized by drought type. *Average duration* refers to mean event duration in days. *Fraction of mean duration* (%) indicates the proportion of each drought type relative to the total mean duration. *Relative bias* (%) is calculated as $(N_{GCM} - N_{EOBS})/N_{EOBS} \times 100$, representing the percentage difference between modelled and observed mean duration. Negative values indicate underestimation by the model.

Metrics	**Rainfall Deficit**	**Rain to Snow**	**Wet to Dry**	**Warm Snow**	**Cold Snow**	**Snowmelt**	**Composite**
EOBS v25 observations							
Mean duration	95.40	141.11	106.73	67.56	66.37	60.46	42.26
Fraction of mean duration (%)	16.5	24.3	18.4	11.7	11.4	10.4	7.3
MIROC							
Mean duration	105.37	217.00	135.43	81.61	75.35	64.83	41.74
Fraction of mean duration (%)	14.61	30.08	18.77	11.31	10.45	8.99	5.79
Relative bias (%)	10.45	53.78	26.88	20.79	13.53	7.22	-1.25
GFDL							
Average duration	119.80	206.16	153.47	81.64	79.70	63.39	38.71
Fraction of mean duration (%)	16.13	27.75	20.66	10.99	10.73	8.53	5.21
Relative bias (%)	25.57	46.10	43.79	20.83	20.07	4.84	-8.42
HadGEM2							
Average duration	109.59	213.11	142.99	64.80	81.45	71.95	94.74
Fraction of mean duration (%)	14.07	27.37	18.36	8.32	10.46	9.24	12.17
Relative bias (%)	14.87	51.03	33.97	-4.09	22.71	19.00	124.18
IPSL							
Average duration	116.54	200.62	115.93	76.19	76.46	76.69	98.35
Fraction of mean duration (%)	15.32	26.37	15.24	10.01	10.05	10.08	12.93
Relative bias (%)	22.16	42.17	8.62	12.77	15.19	26.85	132.72
NorESM							
Average duration	123.64	222.87	129.53	64.47	72.52	67.89	94.31
Fraction of mean duration (%)	15.95	28.75	16.71	8.32	9.35	8.76	12.17
Relative bias (%)	29.60	57.94	21.36	-4.57	9.26	12.29	123.15

Looking at the spatial patterns of drought duration for the historical period (1971–2000), Figure S4a reveal substantial variability across Europe. The EOBS observational dataset indicates particularly long durations (exceeding 120 days) for

Table S2. Comparison of average runoff deficit between GCMs (RCP4.5) and EOBS (1971–2000), categorized by drought type. *Average runoff deficit* refers to mean standardized deficit values. *Fraction of events* (%) indicates the proportion of each drought type relative to the total event count. *Relative bias* (%) is calculated as $(N_{GCM} - N_{EOBS})/N_{EOBS} \times 100$, representing the percentage difference between modelled and observed deficit values. Negative values indicate underestimation by the model.

Metrics	**Rainfall Deficit**	**Rain to Snow**	**Wet to Dry**	**Warm Snow**	**Cold Snow**	**Snowmelt**	**Composite**
EOBS v25 observations							
Mean runoff deficit	-1.86	-3.90	-2.18	-0.84	-1.04	-1.34	-0.69
Fraction of mean runoff deficit (%)	15.7	32.9	18.4	7.1	8.8	11.3	5.8
MIROC							
Mean runoff deficit	-3.78	-11.06	-5.52	-1.35	-2.21	-1.85	-0.92
Fraction of mean runoff deficit (%)	14.18	41.44	20.68	5.05	8.28	6.92	3.45
Relative bias (%)	103.33	183.61	152.76	59.92	112.25	38.01	33.32
GFDL							
Mean runoff deficit	-4.26	-9.89	-5.76	-1.54	-2.24	-1.65	-1.32
Fraction of mean runoff deficit (%)	15.97	37.10	21.60	5.77	8.42	6.19	4.95
Relative bias (%)	128.67	153.50	163.60	82.33	115.65	23.34	91.12
HadGEM2							
Mean runoff deficit	-3.64	-13.03	-5.33	-1.13	-2.16	-2.75	-1.37
Fraction of mean runoff deficit (%)	12.36	44.30	18.12	3.84	7.35	9.36	4.66
Relative bias (%)	95.40	234.12	144.10	34.21	107.54	105.85	98.76
IPSL							
Mean runoff deficit	-4.01	-9.78	-4.15	-1.70	-1.85	-2.37	-2.28
Fraction of mean runoff deficit (%)	15.34	37.41	15.89	6.51	7.06	9.05	8.74
Relative bias (%)	115.56	150.91	90.31	101.93	77.35	76.97	231.05
NorESM							
Mean runoff deficit	-4.83	-14.58	-5.33	-1.19	-2.05	-2.08	-3.93
Fraction of mean runoff deficit (%)	14.22	42.89	15.68	3.50	6.03	6.11	11.57
Relative bias (%)	159.77	273.80	144.08	41.22	96.85	55.28	469.62

rainfall deficit droughts in Mediterranean regions and reaching 90-120 days for rain-to-snow droughts in northern Europe. These patterns reflect distinct hydroclimatic controls on drought persistence, with snow-related processes predominating in the north and rainfall deficits in the south (Brunner et al., 2022). Snow-related drought types (warm snow, cold snow, snowmelt) display shorter durations generally concentrated in mountainous and northern regions, while composite droughts show the most spatially limited occurrence. The ensemble mean of historical GCM simulations (Figure S4b) reproduces the general spatial patterns observed in EOBS data, capturing the north-south gradient in drought duration characteristics. However, models show some amplification of duration patterns, particularly for rainfall deficit droughts in southern Europe and rain-to-snow droughts in northern regions.

Comparison between historical GCM simulations and EOBS observations (GCM_hist – EOBS; Figure S4c) shows relatively sparse and spatially limited differences across most typologies, suggesting that models generally capture mean drought durations reasonably well across much of the continent. The bias patterns reveal that models generally overestimate drought durations across most drought types and regions, with positive biases (yellow-red colors) dominating the spatial patterns, while negative biases are relatively sparse and localized. Regional differences in mean drought duration (Figure S4d) highlight specific model biases. Northern Europe (NEU) exhibits notable positive biases for rain-to-snow droughts, with median differences reaching approximately +50 days, indicating that models tend to overestimate the persistence of snow-related drought events in this region (Fang and Leung, 2023). Interestingly, this contrasts with the simultaneous underestimation of runoff deficit severity in the same region and drought type, pointing to a complex bias structure wherein simulated droughts are less severe but longer-lasting than observed. Mediterranean regions display more moderate biases across drought types. Wet-to-dry transitions, however, show wider interquartile ranges across all regions, suggesting greater uncertainty in modelling soil moisture-driven drought mechanisms in current-generation climate models (Spinoni et al., 2018).

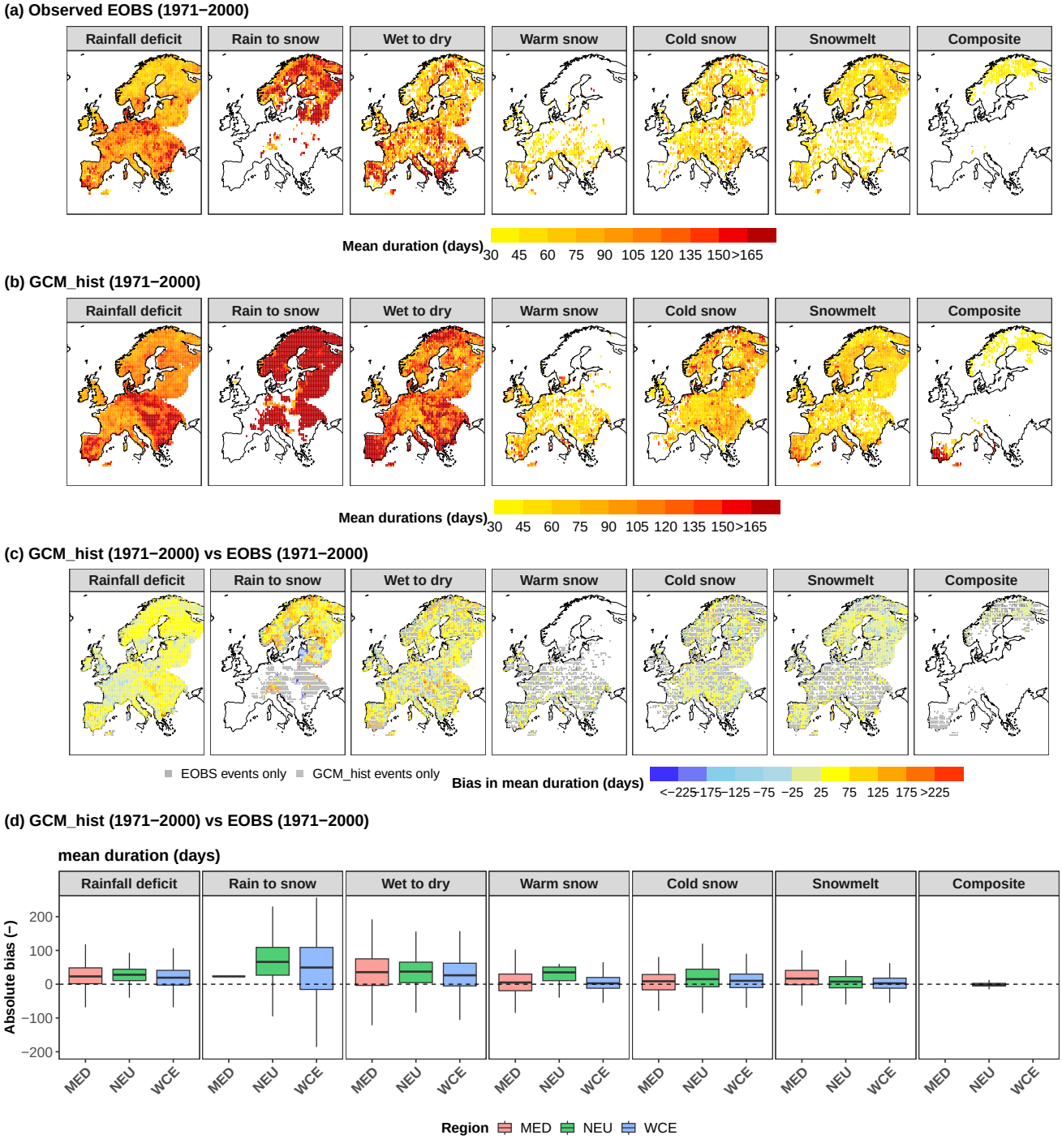

Figure S4. Assessment of bias in mean drought duration (days) for different drought types. (a) observed EOBS data (1971–2000); (b) ensemble mean drought duration for historical GCM simulations (GCM_{hist}, 1971–2000); (c) bias in mean drought duration between GCM_{hist} and EOBS; and (d) absolute bias of mean duration (days) in historical GCM simulations relative to EOBS observations for three IPCC reference regions (MED, NEU, WCE) and each drought type. Results are derived from an ensemble of five GCMs.

The spatial distribution of mean number of drought events across Europe during the historical baseline period (1971–2000) shows pronounced regional heterogeneity, dependent on drought type (Figure S5). Based on the EOBS gridded observational dataset, rainfall deficit droughts occur most frequently in the Mediterranean basin, with local totals often exceeding 11 events over the 30-year period. Central Europe exhibits intermediate event counts, typically between 5 and 9. Droughts associated with rain-to-snow transitions are less frequent and largely confined to northern and orographically elevated regions, consistent with the spatial distribution reported by (Van Loon and Van Lanen, 2012). Temperature-driven drought typologies (e.g. warm snow and cold snow) display more spatially heterogeneous distributions, reflecting the diverse hydroclimatic controls that shape their occurrence across different regions.

A comparison between historical GCM simulations (`GCM_hist`) and EOBS observations reveals systematic biases in the simulated number of events. Most notably, GCMs markedly underestimate rainfall deficit droughts across the Mediterranean and Western-Central Europe, with local differences reaching as much as -9 to -13 events. These discrepancies are consistent with findings by (Roudier et al., 2016), who linked them to the limited skill of GCMs in reproducing regional precipitation variability in semi-arid settings. Boxplot diagnostics indicate median underestimations of approximately -3 events in the Mediterranean (MED) and -4 events in Western-Central Europe (WCE). Conversely, `GCM_hist` simulations overestimate the number of rainfall deficit droughts in Northern Europe (NEU), suggesting a latitudinal bias in model performance. For wet-to-dry transitions, GCMs exhibit a consistent positive bias across all subregions, corroborating the results of (Seneviratne et al., 2010; Berg et al., 2016), who highlighted persistent difficulties in modelling soil moisture dynamics in current-generation climate models.

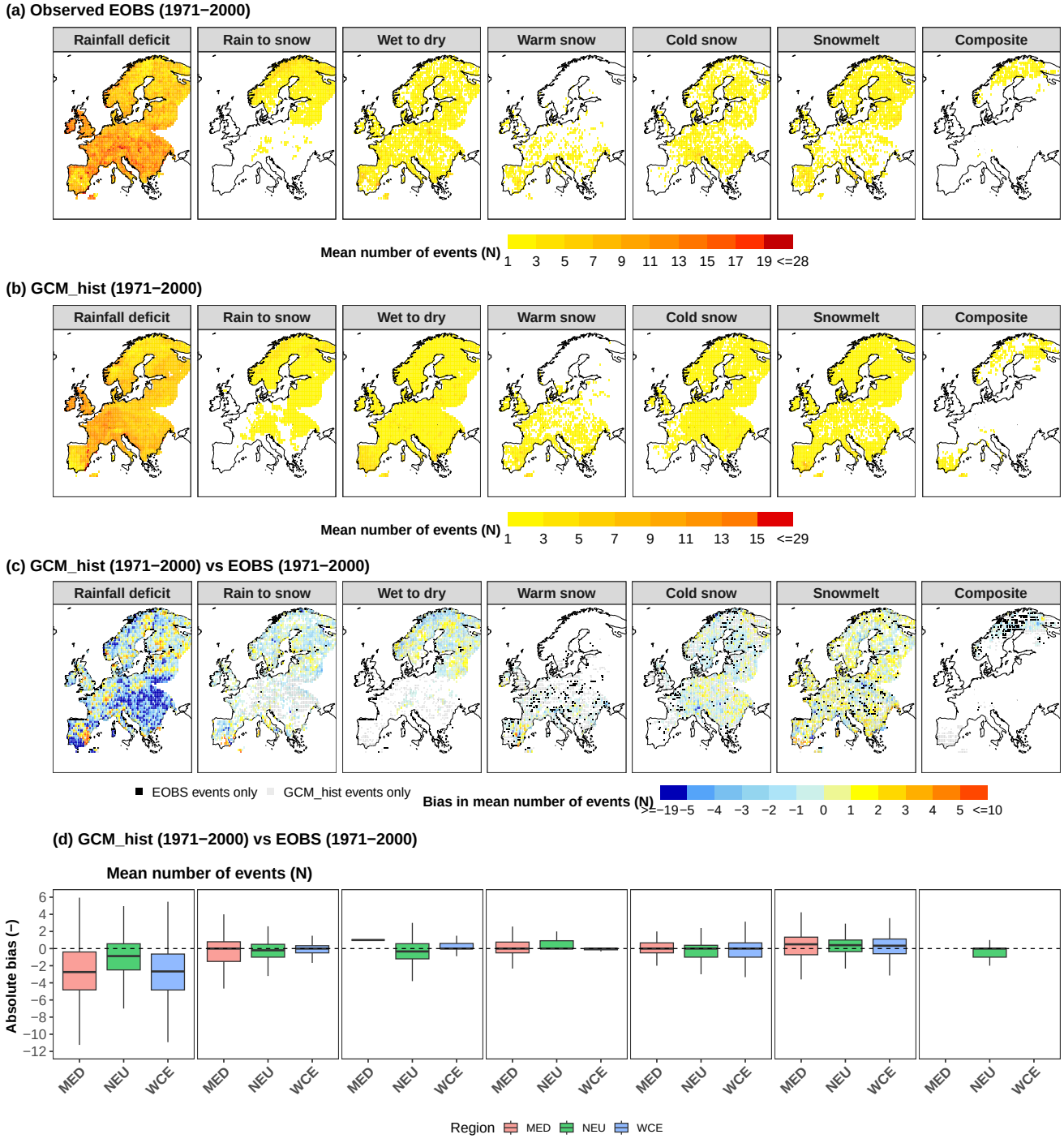

Figure S5. Assessment of bias in mean number of events (–) for different drought types. (a) observed EOBS data (1971–2000); (b) ensemble mean number of events for historical GCM simulations (GCM_{hist}, 1971–2000); (c) bias in mean number of events between GCM_{hist} and EOBS; and (d) absolute bias of mean number of events in historical GCM simulations relative to EOBS observations for three IPCC reference regions (MED, NEU, WCE) and each drought type. Results are derived from an ensemble of five GCMs.

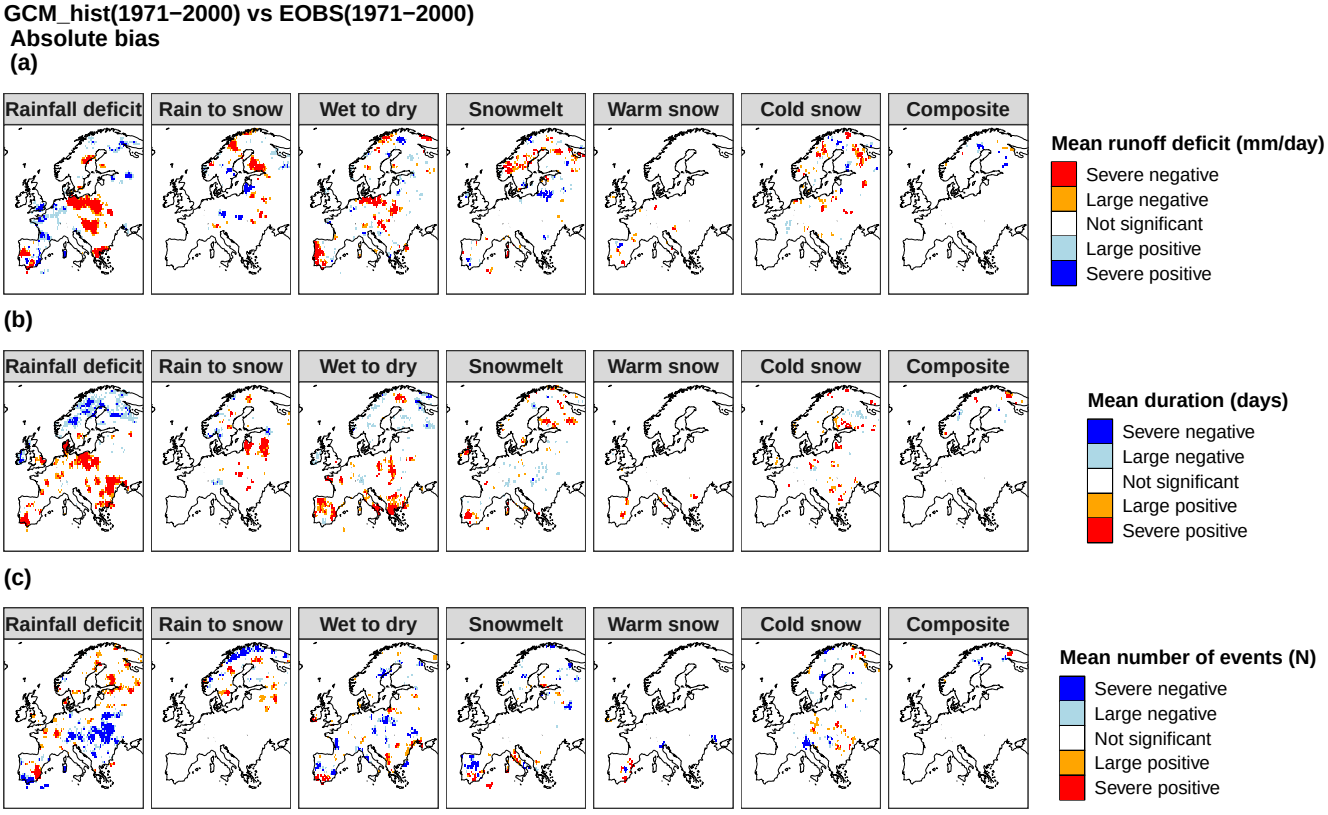

Figure S6. Getis-Ord Gi* hotspot analysis of absolute bias in historical GCM simulations (`GCM_hist`, 1971–2000) relative to EOBS observations (1971–2000) across European grid cells, disaggregated by drought type. Panels show spatial clusters of bias in (a) mean runoff deficit (mm day^{-1}), (b) mean drought duration (days), and (c) mean number of drought events. Colours indicate statistically significant positive and negative bias clusters, with darker tones representing more severe bias magnitudes.

Figure S6 presents the results of a Getis-Ord Gi* hotspot analysis, illustrating spatial clusters of absolute bias in drought characteristics across different drought types for the historical period (GCM_hist vs. EOBS, 1971–2000). The analysis reveals distinct regional patterns of model bias across Europe.

For mean runoff deficit (mm day^{-1}), extensive severe and large negative clusters, indicating underestimation by models, are observed over northern and central Europe, particularly for rainfall deficit and snow-related drought types. Localised positive hotspots, indicative of overestimation, appear in parts of the Mediterranean region. These regional discrepancies highlight persistent limitations in the models' capacity to simulate key hydrological processes (Hagemann et al., 2011; Maraun et al., 2010).

Bias patterns in mean drought duration show widespread negative clustering in northern Europe, especially for rainfall deficit droughts, suggesting an underestimation of drought persistence. This may reflect model limitations in reproducing slow-evolving hydrometeorological conditions and land–atmosphere feedback mechanisms (van der Linden and Mitchell, 2009).

The most striking biases emerge in the mean number of drought events, with large negative clusters across Europe. This widespread underestimation of drought frequency spans multiple drought types, pointing to fundamental challenges for GCMs in capturing the temporal structure of drought occurrence (Doblas-Reyes et al., 2013). Collectively, these results underscore systematic deficiencies in GCM performance, particularly in representing drought frequency and persistence in northern Europe.

References

Berg, A., Findell, K., Lintner, B., Giannini, A., Seneviratne, S. I., Van Den Hurk, B., Lorenz, R., Pitman, A., Hagemann, S., Meier, A., et al.: Land–atmosphere feedbacks amplify aridity increase over land under global warming, Nature Climate Change, 6, 869–874, 2016.

Brunner, M. I., Van Loon, A. F., and Stahl, K.: Moderate and severe hydrological droughts in Europe differ in their hydrometeorological drivers, Water Resources Research, 58, e2022WR032 871, 2022.

Doblas-Reyes, F. J., García-Serrano, J., Lienert, F., Biescas, A. P., and Rodrigues, L. R.: Seasonal climate predictability and forecasting: status and prospects, Wiley Interdisciplinary Reviews: Climate Change, 4, 245–268, 2013.

Fang, Y. and Leung, L. R.: Northern hemisphere snow drought in Earth system model simulations and ERA5-land data in 1980–2014, Journal of Geophysical Research: Atmospheres, 128, e2023JD039 308, 2023.

Hagemann, S., Chen, C., Haerter, J. O., Heinke, J., Gerten, D., and Piani, C.: Impact of a statistical bias correction on the projected hydrological changes obtained from three GCMs and two hydrology models, Journal of Hydrometeorology, 12, 556–578, 2011.

Maraun, D., Wetterhall, F., Ireson, A. M., Chandler, R. E., Kendon, E. J., Widmann, M., Brienen, S., Rust, H. W., Sauter, T., Themeßl, M., et al.: Precipitation downscaling under climate change: Recent developments to bridge the gap between dynamical models and the end user, Reviews of geophysics, 48, 2010.

Roudier, P., Andersson, J., Donnelly, C., Feyen, L., Greuell, W., and Ludwig, F.: Projections of future floods and hydrological droughts in Europe under a+ 2 C global warming, Climatic change, 135, 341–355, 2016.

Seneviratne, S. I., Corti, T., Davin, E. L., Hirschi, M., Jaeger, E. B., Lehner, I., Orlowsky, B., and Teuling, A. J.: Investigating soil moisture–climate interactions in a changing climate: A review, Earth-Science Reviews, 99, 125–161, 2010.

Spinoni, J., Vogt, J. V., Barbosa, P., Dosio, A., McCormick, N., Bigano, A., and Füssel, H.-M.: Changes of heating and cooling degree-days in Europe from 1981 to 2100, Int. J. Climatol, 38, e191–e208, 2018.

van der Linden, P. and Mitchell, JFB, e.: ENSEMBLES: Climate Change and its Impacts: Summary of research and results from the ENSEMBLES project, Met Office Hadley Centre, FitzRoy Road, Exeter EX1 3PB, UK, 160, 2009.

Van Loon, A. F. and Van Lanen, H. A.: A process-based typology of hydrological drought, Hydrology and Earth System Sciences, 16, 1915–1946, 2012.